REPORT DOCUMENTATION PAGE

Form Approved OMB No. 0704-0188

1. REPORT DATE *(DD-MM-YYYY)*	2. REPORT TYPE	3. DATES COVERED *(From - To)*
30-Sep-2009	REPRINT	

4. TITLE AND SUBTITLE
HIGH-RESOLUTION SEISMIC VELOCITY AND ATTENUATION MODELS OF THE CAUCASUS-CASPIAN REGION

5a. CONTRACT NUMBER
FA8718-07-C-0007

5b. GRANT NUMBER

5c. PROGRAM ELEMENT NUMBER
62601F

6. AUTHOR(S)
Robert J. Mellors[1], Rengin Gök[2], Michael E. Pasyanos[2], Gleb Skobeltsyn[3], Eric Sandvol[3], Ugur Teoman[4], Gurban Yetirmishli[5] and Tea Godoladze[6]

5d. PROJECT NUMBER
1010

5e. TASK NUMBER
SM

5f. WORK UNIT NUMBER
A1

7. PERFORMING ORGANIZATION NAME(S) AND ADDRESS(ES)
San Diego State University
5500 Campanille Drive
San Diego, CA 92182-7426

8. PERFORMING ORGANIZATION REPORT NUMBER

9. SPONSORING / MONITORING AGENCY NAME(S) AND ADDRESS(ES)
Air Force Research Laboratory
29 Randolph Road
Hanscom AFB, MA 01731-3010

10. SPONSOR/MONITOR'S ACRONYM(S)
AFRL/RVBYE

11. SPONSOR/MONITOR'S REPORT NUMBER(S)
AFRL-RV-HA-TR-2009-1071

12. DISTRIBUTION / AVAILABILITY STATEMENT
Approved for Public Release; Distribution Unlimited.

San Diego State University[1], Lawrence Livermore National Laboratory[2], University of Missouri-Columbia[3], Kandilli Observatory and Earthquake Research Institute, Turkey[4], Azerbaijan Republic Seismic Survey[5] and Seismic Monitoring Center, Georgia[6]

13. SUPPLEMENTARY NOTES
Reprinted from: Proceedings of the 2009 Monitoring Research Review – Ground-Based Nuclear Explosion Monitoring Technologies, 21 – 23 September 2009, Tucson, AZ, Volume I pp 150 - 157.

14. ABSTRACT

The Caucasus-Caspian region is part of the Alpine-Himalayan collision belt and is an area of complex structure accompanied by large variations in seismic wave velocities. Using data from 29 new broadband seismic stations in the region as well as data from a temporary (1999-2001) deployment in eastern Turkey, a unified velocity structure is developed using teleseismic receiver functions and surface waves. Joint inversion of surface wave group dispersion curves generated from ambient noise with receiver functions show that crustal thickness varies from 34 to 52 km in the region. The thickest crust is in Lesser Caucasus and the thinnest is in the Arabian Plate. Thin crust is also observed near the Caspian. The lithospheric mantle in the Greater Caucasus and the Kura depression is faster than the Anatolian Plateau and Lesser Caucasus. This possibly indicates the presence of cold lithosphere. The lower crust is slowest in the northeastern part of the Anatolian Plateau where Holocene volcanoes are located. Fundamental mode Rayleigh wave phase velocities are determined at periods between 20 and 145 seconds. We observe a relatively high-velocity zone located in the upper mantle under the Kura basin and the western part of Caspian Sea that is continuous to the Moho. The images show very low velocities beneath the eastern Anatolian plateau implying the existence of a partially molten asthenospheric material underlying a very thin lithosphere. Using a two-station method, both *Lg* and *Pg* attenuation is measured and tomographically inverted to yield attenuation maps. Efficient *Lg* propagation is observed throughout much of the Arabian plate. Moderate *Lg* Q is observed in the Lesser Caucasus and Kura Basin while low *Lg* Q is observed in the East Anatolian plateau. *Pg* shows highly variable propagation throughout the region.

15. SUBJECT TERMS
Seismic velocity models, Surface waves, Middle East

16. SECURITY CLASSIFICATION OF:			17. LIMITATION OF ABSTRACT	18. NUMBER OF PAGES	19a. NAME OF RESPONSIBLE PERSON
a. REPORT	b. ABSTRACT	c. THIS PAGE			Robert J. Raistrick
UNCLAS	UNCLAS	UNCLAS	SAR	8	19b. TELEPHONE NUMBER *(include area code)*

HIGH-RESOLUTION SEISMIC VELOCITY AND ATTENUATION MODELS OF THE CAUCASUS-CASPIAN REGION

Robert J.Mellors[1], Rengin Gök[2], Michael E. Pasyanos[2], Gleb Skobeltsyn[3], Eric Sandvol[3], Ugur Teoman[4], Gurban Yetirmishli[5], and Tea Godoladze[6]

San Diego State University[1], Lawrence Livermore National Laboratory[2], University of Missouri-Columbia[3], Kandilli Observatory and Earthquake Research Institute, Turkey[4], Azerbaijan Republic Seismic Survey[5], and Seismic Monitoring Center, Georgia[6]

Sponsored by the Air Force Research Laboratory

Award No. FA8718-07-C-0007
Proposal No. BAA07-18

ABSTRACT

The Caucasus-Caspian region is part of the Alpine-Himalayan collision belt and is an area of complex structure accompanied by large variations in seismic wave velocities. Using data from 29 new broadband seismic stations in the region as well as data from a temporary (1999-2001) deployment in eastern Turkey, a unified velocity structure is developed using teleseismic receiver functions and surface waves. Joint inversion of surface wave group dispersion curves generated from ambient noise with receiver functions show that crustal thickness varies from 34 to 52 km in the region. The thickest crust is in Lesser Caucasus and the thinnest is in the Arabian Plate. Thin crust is also observed near the Caspian. The lithospheric mantle in the Greater Caucasus and the Kura depression is faster than the Anatolian Plateau and Lesser Caucasus. This possibly indicates the presence of cold lithosphere. The lower crust is slowest in the northeastern part of the Anatolian Plateau where Holocene volcanoes are located. Fundamental mode Rayleigh wave phase velocities are determined at periods between 20 and 145 seconds. We observe a relatively high-velocity zone located in the upper mantle under the Kura basin and the western part of Caspian Sea that is continuous to the Moho. The images show very low velocities beneath the eastern Anatolian plateau implying the existence of a partially molten asthenospheric material underlying a very thin lithosphere. Using a two-station method, both *Lg* and *Pg* attenuation is measured and tomographically inverted to yield attenuation maps. Efficient *Lg* propagation is observed throughout much of the Arabian plate. Moderate *Lg* Q is observed in the Lesser Caucasus and Kura Basin while low *Lg* Q is observed in the East Anatolian plateau. *Pg* shows highly variable propagation throughout the region.

OBJECTIVES

The objective of the research is to develop 3D seismic velocity structure and regional phase attenuation models for the Caucasus-Caspian region (Figure 1). Specifically, the purpose of this work was to:

- Create upper mantle/crustal velocity models using data from new stations in the region.
- Construct detailed maps of regional phase attenuation.
- Compare and validate results and models using the various algorithms as well as independent datasets

The work consisted of four main tasks: data collection, regional phase analysis, crustal and upper mantle velocity determination, and model validation.

RESEARCH ACCOMPLISHED

Data collection. Waveform data was collected from 33 stations (Figure 1) in the region as part of collaborative effort with the individual seismic surveys. The primary focus was collecting continuous data from 2006-2008, although waveform data from other years was collected as available. All data has been provided to the Knowledge Base at Lawrence Livermore National Laboratory.

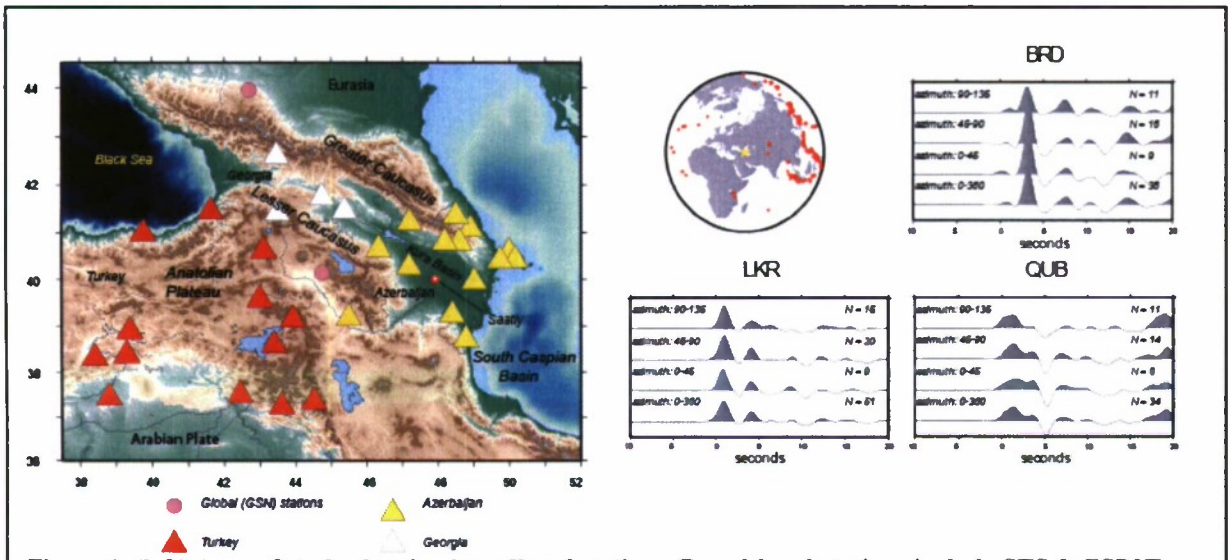

Figure 1. (left) Area of study showing broadband stations. Broad-band stations include STS-2, ESP3T, ESP3ESD and CMG40T type instruments.(right) Example receiver functions stacked by back-azimuth for selected Azerbaijan stations. Global map shows recorded events (red dots) and location of stations (yellow star). Small red circle shows position of Saatly 8 km deep well used for model validation.

Surface wave group velocity and receiver function joint inversion. To develop a comprehensive model of crustal and upper mantle velocities, joint inversion of receiver functions and surface waves was applied. Crustal receiver functions are sensitive to velocity discontinuities while surface wave dispersion is controlled by average S-wave velocity structure (e.g. Julia et al., 2000). Therefore, combining the two methods yields a robust estimate of crustal and upper mantle velocities. Receiver functions using events at distances between 30 and 90 degrees were calculated for all stations using iterative deconvolution at Gaussian widths of 1.0, 1.5, and 2.5 seconds. Each receiver function (Figure 1) was examined for consistency and signals with excessive amplitudes on the tangential component or grossly different from the stacked average for each station was discarded. Coverage was best for back-azimuths to the east and sparse to the west. Initially, the receiver functions were modeled independently to investigate quality. The slant stacking of Zhu and Kanamori (2000) was also used to estimate Moho depths. In general, the stations near the Caspian show poor quality receiver functions with indications of considerable crustal scattering and reverberations due to the thick sediments. These were difficult to model. Some indications of 3D structure were observed for stations in the Greater Caucasus as the receiver functions showed clear variations with back azimuth.

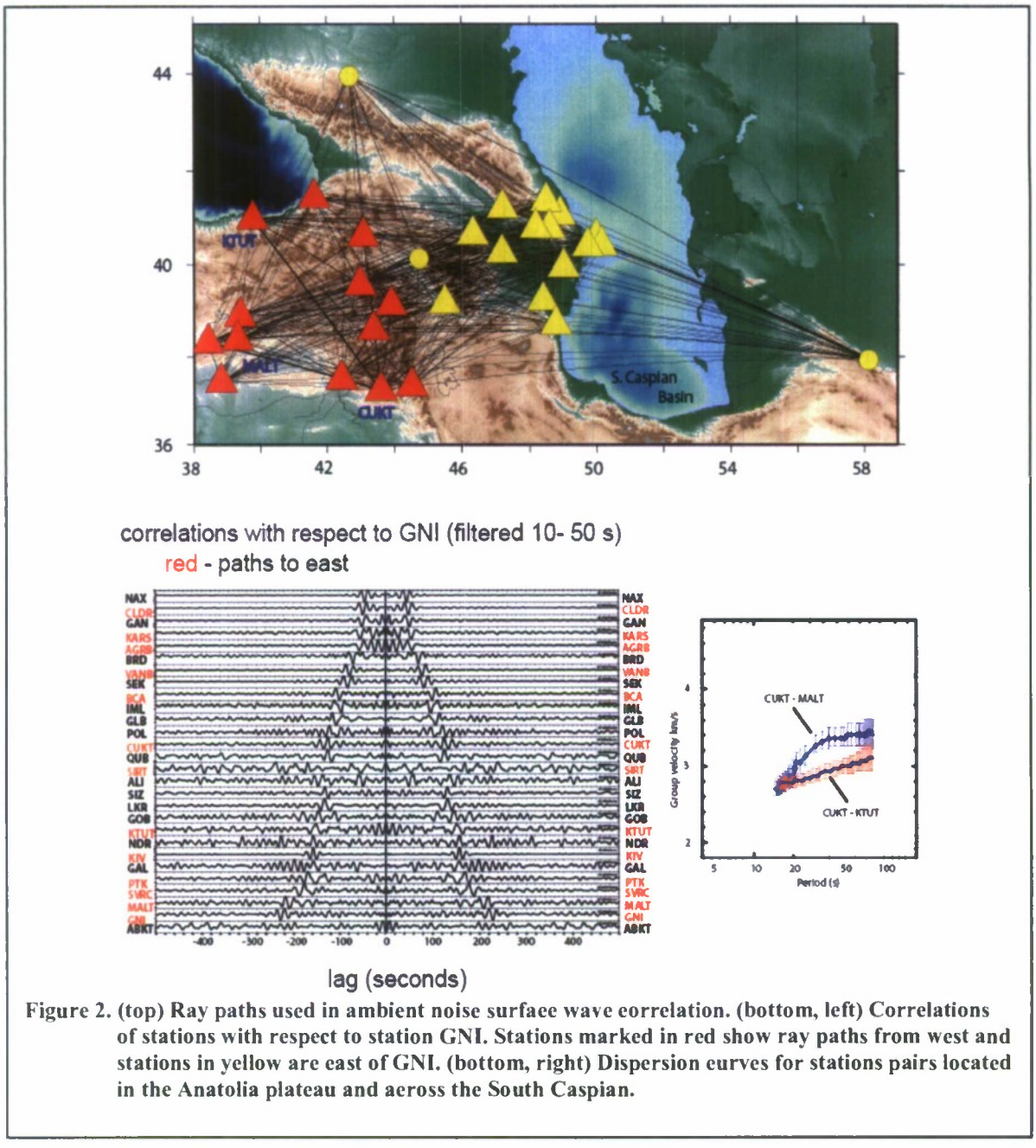

Figure 2. (top) Ray paths used in ambient noise surface wave correlation. (bottom, left) Correlations of stations with respect to station GNI. Stations marked in red show ray paths from west and stations in yellow are east of GNI. (bottom, right) Dispersion curves for stations pairs located in the Anatolia plateau and across the South Caspian.

Surface wave group velocity dispersion measurements were made using both event-based and ambient noise correlation methods. Love and Rayleigh wave group velocity dispersion curves were estimated for over 1,500 waveforms at periods of 7–100 sec. Ambient noise correlation was applied to all possible station pairs (~400) to obtain Rayleigh wave group velocities. All dispersion curves were picked manually and then included in the global/regional tomographic inversion of Pasyanos et al. (2005). We then extracted the dispersion curves from the tomography maps of surface waves and combined them with stacked receiver functions.

Horizontal depth slices of 11, 35 and 87 km are shown in Figure 3 as well as an estimated Moho thickness map. The thick sediments of Kura Basin are evident in upper crust with low velocities averaging Vs=2.8 km/s. The eastern part of the Greater Caucasus shows similar low velocities in the upper crust. The slowest lower crustal velocities are observed in the northeastern Anatolian plateau and Lesser Caucasus region where considerable Neogene/Quaternary, Holocene volcanic activity has occurred. Faster lower crustal velocities occur at the edge of

the Caspian and in the Arabian plate. The upper mantle appears distinctly slow under the Anatolian plateau and to the southeast. Indications of faster upper mantle velocities occur under the Greater Caucasus. It was noted that inversion for Love and Rayleigh waves provided slightly different results, possibly due to anisotropy.

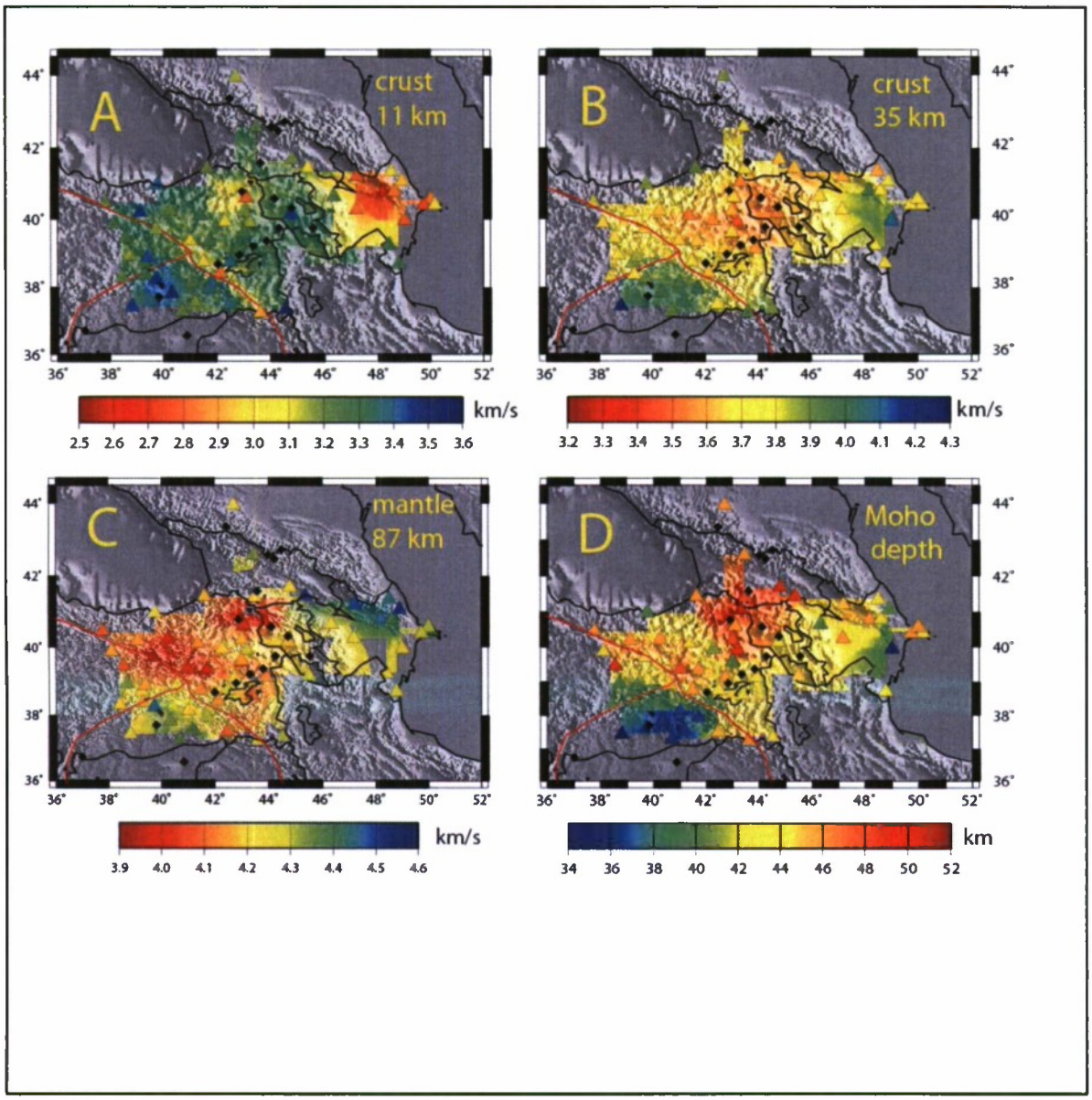

Figure 3. A, B) Crustal S velocities estimated from joint inversion at depths of 11 (left) and 35.5 km (right). C) Upper mantle S velocities at a depth of 87 km. D) Moho depth inferred from velocity profiles based from joint inversion. Black lines mark international borders and coastlines; red lines show major faults and suture zones. Black dots are Holocene volcanics.

Surface wave phase velocity inversion. To investigate variations in upper mantle velocities, surface wave phase velocities measured from earthquakes were also inverted. Data from an earlier temporary deployment of 29 stations was used as well as the newer data. Teleseismic earthquakes with a magnitude greater than 5.8 were selected and the waveforms were evaluated for high signal to noise at the longer periods (50 and 125 seconds). Unfortunately, many of the Azerbaijan stations showed high noise levels at the longer periods even on the vertical component, possibly due to barometric variations. This restricted the data set to 20 events. The data for each event were filtered to create 13 frequency bands with corresponding centered periods ranging from 20 to 145 seconds and dispersion curves were

estimated from these results. Initially, the Rayleigh wave phase dispersion was inverted to estimate 1D velocities. The results were topographically inverted for 2D structure on a 50 km grid using two methods: Forsyth et al. (1998) and Yang and Forsyth (2006). The two methods are similar but the Yang and Forsyth technique attempts to compensate for scattering caused by local heterogeneities and therefore should improve spatial resolution (Figure 4). The results at shorter wavelengths were more robust than for the longer wavelengths especially for the area covered by the Azeri stations, possibly due to excessive noise at longer wavelengths. Higher upper mantle velocities were observed under Anatolia and lower velocities under the Caucasus/Caspian.

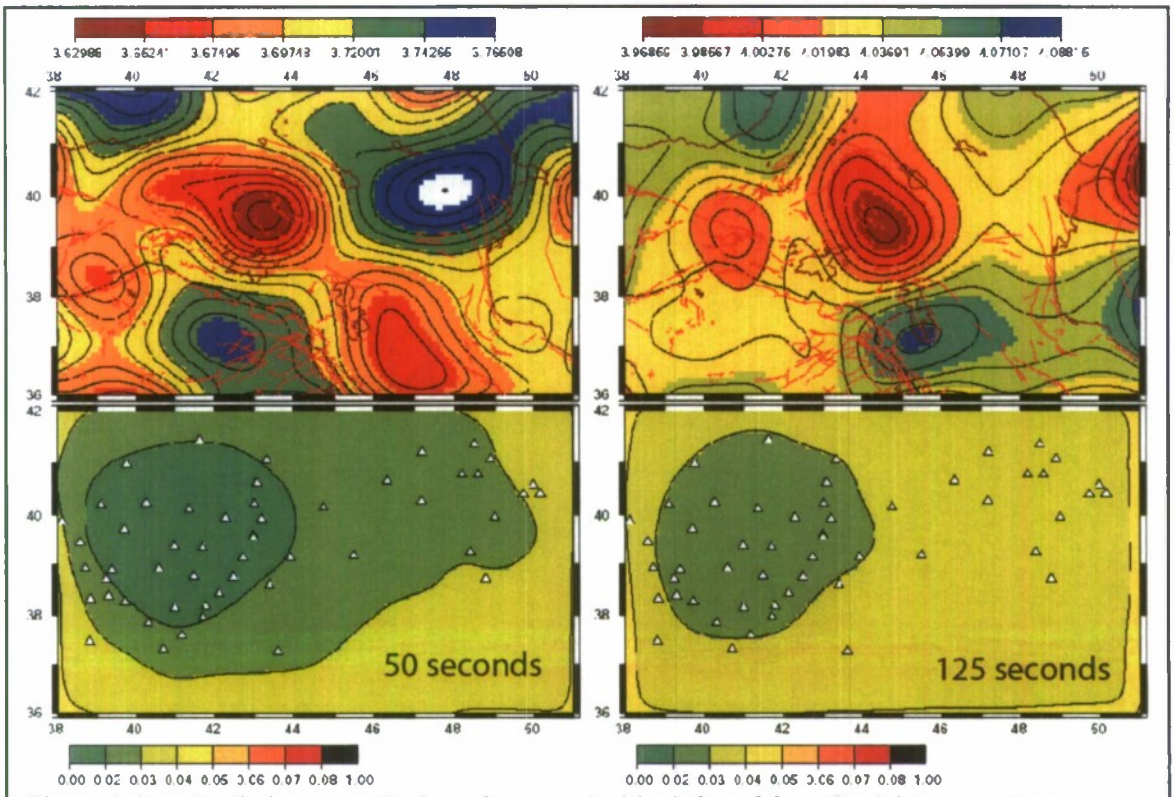

Figure 4. (top) Preliminary results from S wave velocities inferred from Rayleigh wave phase dispersion at periods of 50 (left) and 125 seconds (right). The method of Yang and Forsyth (2006) was used. The lower plots show the estimated errors in units of velocity with triangles denoting station locations. Due to high noise at longer periods, results from the Caucasus at longer periods are not well constrained.

Regional phase analysis. The purpose of the regional phase analysis was to extend regional phase attenuation maps (e.g., Al-Lazki et al., 2003; Gok et al., 2003) throughout Anatolia and the Caucasus (Figure 5). The mapping was performed by first measuring attenuation between stations and then inverting to solve for the average Q in discrete spatial cells. The direct two-station method was used (e.g., Zor et al., 2007; Xie et al., 2004) to estimate attenuation for each path. This method relies on spectral ratios between pairs of station aligned with the ray paths from each event. Phases were identified manually to avoid problems caused by variations in crustal velocities. Spectra for each phase were estimated after windowing. Station pairs for each event were selected using a criteria based on inter-station distance and alignment with event (±15°). The spectral ratio between two stations was calculated for appropriate station pairs after correction for distance (Xie et al., 2004) and geometrical spreading. Q and η (frequency dependence) were then estimated from the spectral ratios using linear regression. This Q and η represents the attenuation along a line between the two stations. These attenuation measurements were added to an existing Middle East dataset which was inverted to create a regional map (Figure 5). The dataset includes approximately 3000 station pairs. Separate inversions were conducted for both *Lg* and *Pg*. Checkerboard tests were performed to evaluate resolution and both ART and LSQR inversion algorithms were tested to evaluate the effect of possible numerical artifacts. Results were similar for both algorithms. Raypath coverage is good in eastern Anatolia but is sparser towards the Caucasus and Caspian.

The 1 Hz *Lg* results show a broad zone of high attenuation (low Q) extending roughly east-west north of the Arabian plate from Anatolia to the Caspian (Figure 5). Considerable spatial variation exists which likely reflects the complicated tectonics. *Lg* appears to propagate well in the Arabian plate but is dramatically attenuated in the Lesser Caucasus. This may be due to the volcanism and the possibility of partial melt in the crust. The Kura basin and the extreme eastern Caucasus show moderate to low attenuation, which may reflect the influence of the Eurasia plate. It is clear from these results that the Kura basin is underlain by continental crust and is distinct from the South Caspian. The variations in *Lg* attenuation appear to result from a combination of both crustal heterogeneity and changes in crustal thickness. While Moho depth increases by 5 to 10 km at the northern edge of the Arabian Plate the variation in depth from Anatolia to the Lesser Caucasus is fairly small and yet relatively low *Lg* Q is observed. Volcanic regions are often observed to possess low Lg Q possibly due to high attenuation of shear waves by partial melt in the crust. *Pg* reveals a distinctly different pattern. The transition between the Arabian plate and Anatolian plateau is defined by an abrupt change in *Pg* Q east of about 38 E longitude but a clear zone of high Q exists in the Lesser Caucasus. The zone of low Q along the Caspian and Kura basin may be caused by the abrupt thickening in sediments and dipping Moho, which decreases the efficiency of the crustal *P* waveguide.

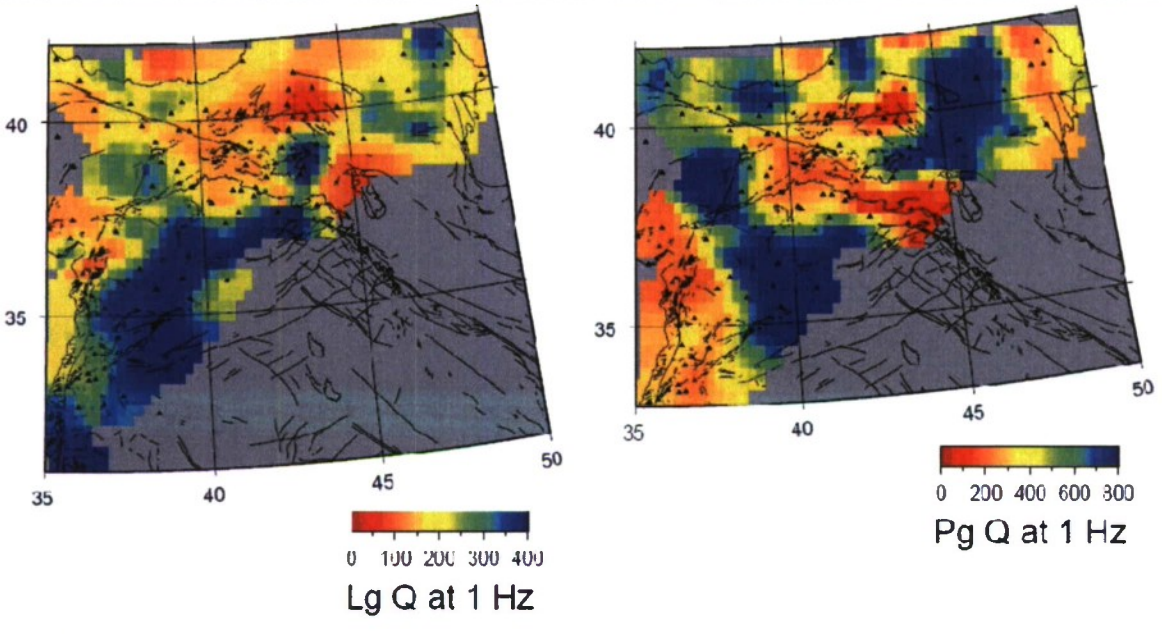

Figure 5. Attenuation maps for *Lg* (left) and *Pg* (right).

Model validation. The model was tested in several ways: comparison with alternate datasets such as reflection seismic and gravity, earthquake hypocenters comparison, and with waveform modeling. Seismic reflection refraction data shows clearly the deep sedimentary layers in the South Caspian and coastline (Knapp et al., 2004; Mangino and Priestley, 1998). Gravity data also suggests deep basement, which closely matches the low velocitics for the area observed by the joint inversion. The Moho depths inferred by refraction data are also similar. 2D modeling of gravity data through the center of the Kura basin shows a clear gravity high that runs roughly north-south and parallel to the Caspian coast and delineates the Kura from the South Caspian. The existence of this basement high is confirmed by the Saatly deep well, which penetrated to a depth of 9 km through a succession of sediment and then volcanoclastic layers. To first order, alternate datasets are consistent with our results, both for crustal and mantle velocities and with phase propagation.

A second set of tests was conducted with earthquake locations. This effort was focused in the Azerbaijan region. The 3D model was averaged to produce an average 1d model. Hypocenter locations were calculated using this model and compared with global PDE (Preliminary Determination of Epicenters) locations. Significant differences in location were observed (up to 30 km) (Figure 6). A major factor is the exceptionally thick sedimentary package in Kura Basin and nearby South Caspian Basin. Waveforms for events with known focal mechanisms were also calculated using this model.

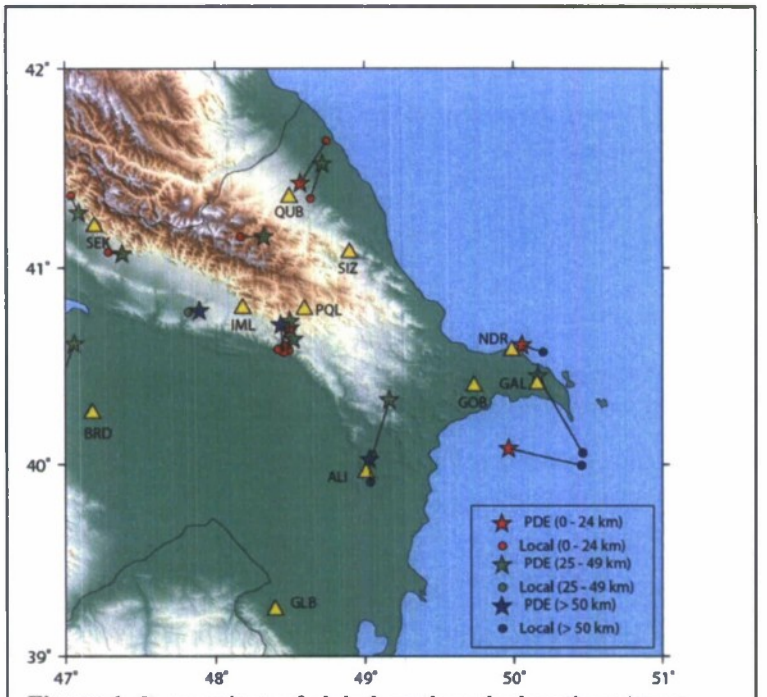

Figure 6. Comparison of global earthquake locations (stars, PDE) with locations determined using the local network (circles) with the new velocity model. Red is shallower than 25 km, green between 25 and 50, and blue is deeper than 50 km. Lines connect different locations of the same event.

CONCLUSIONS AND RECOMMENDATIONS

An improved crustal and upper mantle velocity and attenuation model has been developed for the Caucasus/Caspian region and Anatolian plateau. The Caspian and Kura basins show pronounced low velocities in the upper crust but slightly elevated lower crustal velocities. Crustal thickness varies from about 50 km in the Lesser Caucasus to 35 km in the Arabian plate. The upper mantles display strong heterogeneities in the region. It is slow under the Anatolian plateau and slightly fast under the Greater Caucasus. These are likely related to slab remnants and ongoing volcanism.

Striking variations in regional phase propagation and velocities are mapped. *Lg* is highly attenuated not only in the South Caspian and Black Sea basins but also in the Anatolian plateau, possibly due to a combination of crustal properties under the volcanic areas and varying crustal thickness. A clear change in *Lg* attenuation occurs at the northern edge of the Arabian plate. A narrow band of moderate *Lg* attenuation exists in the Kura basin and along the Caspian. *Pg* also shows variations in attenuation.

Due to the strong spatial variations in both crustal and mantle properties, regional seismic waves should be expected to vary significantly both in travel-time and amplitude in this region. More seismic stations are scheduled to be installed in the region by the various surveys and this data would be useful in increasing the resolution of these results.

ACKNOWLEDGEMENTS

We thank all members of the Kandilli, Georgian, and Azerbaijan seismic surveys for their assistance in gathering data. R. Herrman, C. Ammon, J. Xie, Y. Yang, and J. Julia provided software used in the analysis of this data.

REFERENCES

Al-Lazki, A.I., D. Seber, E. Sandvol, E.,N. Turkelli, R. Mohamad, and M. Barazangi (2003). Tomographic Pn velocity and anisotropy structure beneath the Anatolian plateau (eastern Turkey) and the surrounding regions, *Geophys. Res. Lett.* 30: (24).

Forsyth, D. W., S. C. Webb, L. M. Dorman, and Y. (1998). Phase velocities of Rayleigh waves in the MELT experiment on the East Pacific Rise, *Science* 280: 1235–1238.

Gök R., E. Sandvol, N. Türkelli, D. Seber, and M. Barazangi (2003). *Sn* attenuation in the Anatolian and Iranian plateau and surrounding regions, *Geophys. Res. Lett.* 30: 24, 8042.

Julia, J., C. Ammon, R. Herrman, and A. Correig (2000). Joint inversion of receiver function and surface wave dispersion observations, *Geophys. J. Int.* 143: 1, 99–112.

Knapp, C., J. Knapp, and J. A. Connor (2004). Crust-scale structure of the South Caspian Basin revealed by deep seismic reflection profiling, *Marine and Petro. Geol.* 21: 1073–1081.

Mangino, S and K. Priestley (1998). The crustal structure of the southern Caspian region, *Geophys. J. Inter.* 133: (3), 630–648.

Pasyanos, M. E. (2005). A variable resolution surface wave dispersion study of Eurasia, North Africa, and surrounding regions, *J. Geophys. Res.* 110: B12301, doi: 10.1029/2005JB003749.

Yang, Y. and D. W. Forsyth (2006). Regional tomographic inversion of the amplitude and phase of Rayleigh waves with 2-D sensitivity kernels, *Geophys. J. Int* 166: 1148–1160.

Xie, J., R. Gok, J. Ni, and Y. Aoki (2004). Lateral variations of crustal seismic attenuation along the INDEPTH profiles in Tibet from Lg Q inversion, *J. Geophys. Res.* 109: B10308, doi 10.1029/2004JB002988.

Zhu, L., and H. Kanamori, (2000). Moho depth variation in Southern California from teleseismic receiver functions, *J. Geophys. Res.* 105: (2), 2969–2980.

Zor, E., E. Sandvol, J. Xie, N. Tu¨rkelli, B. Mitchell, A. H. Gasanov, and G. Yetirmishli (2007). Crustal attenuation within the Turkish Plateau and surrounding regions, *Bull. Seismo. Soc. Am.* 97: 1B, 151–161.